BIOCHEMISTRY
including biophysical chemistry & molecular biology
Article

Biochemistry **2010,** *49,* 10179–10186 10179
DOI: 10.1021/bi101465n

Kinetic Basis of Sugar Selection by a Y-Family DNA Polymerase from *Sulfolobus solfataricus* P2[†]

Shanen M. Sherrer,[‡,§] David C. Beyer,[‡] Cynthia X. Xia,[∥] Jason D. Fowler,[‡] and Zucai Suo*[,‡,§]

[‡]*Department of Biochemistry,* [§]*Ohio State Biochemistry Program, and* [∥]*Department of Chemistry, The Ohio State University, Columbus, Ohio 43210, United States*

Received September 9, 2010; Revised Manuscript Received October 12, 2010

ABSTRACT: DNA polymerases use either a bulky active site residue or a backbone segment to select against ribonucleotides in order to faithfully replicate cellular genomes. Here, we demonstrated that an active site mutation (Y12A) within *Sulfolobus solfataricus* DNA polymerase IV (Dpo4) caused an average increase of 220-fold in matched ribonucleotide incorporation efficiency and an average decrease of 9-fold in correct deoxyribonucleotide incorporation efficiency, leading to an average reduction of 2000-fold in sugar selectivity. Thus, the bulky side chain of Tyr12 is important for both ribonucleotide discrimination and efficient deoxyribonucleotide incorporation. Other than synthesizing DNA as the wild-type Dpo4, the Y12A Dpo4 mutant incorporated more than 20 consecutive ribonucleotides into primer/template (DNA/DNA) duplexes, suggesting that this mutant protein possesses both a DNA-dependent DNA polymerase activity and a DNA-dependent RNA polymerase activity. Moreover, the binary and ternary crystal structures of Dpo4 have revealed that this DNA lesion bypass polymerase can bind up to eight base pairs of double-stranded DNA which is entirely in B-type. Thus, the DNA binding cleft of Dpo4 is flexible and can accommodate both A- and B-type oligodeoxyribonucleotide duplexes as well as damaged DNA.

DNA polymerases play critical roles in genomic replication, DNA damage repair, and DNA lesion bypass *in vivo*. To maintain genomic stability, cellular DNA polymerases are required to select correct deoxynucleotides (dNTPs)[1] and to discriminate against both incorrect dNTPs and ribonucleotides (rNTPs) during DNA synthesis. Incorporations of rNTPs lead to DNA strand breakage, genetic mutation, and cell death while dNTP misincorporations result in mutation. Since the cellular concentration of rNTPs is at least 10-fold higher than that of dNTPs (*1*−*3*), DNA polymerases, which are phylogenetically grouped into A, B, C, D, X, Y, and reverse transcriptase (RT) families (*4*), possess efficient mechanisms to limit rNTP binding and incorporation during DNA polymerization. For example, most DNA polymerases and reverse transcriptases (RTs) discriminate against rNTPs by using the steric clash between a bulky side chain of an active site amino acid residue and the ribose 2′-OH of an incoming rNTP (*5*). Through site-directed mutagenesis and kinetic studies, the bulky active site amino acid residue, or "steric gate", has been identified to be either Glu for the A-family polymerases (*6*, *7*) or Tyr (or Phe) for the B-, Y-, and RT-family members (*7*−*14*). Consistently, X-ray crystal structures of the ternary complexes (E·DNA·dNTP) of several DNA polymerases have revealed that the side chain of the "steric gate" residue and the ribose 2′ position of an incoming dNTP are too close to each other and cannot tolerate the presence of a 2′-OH moiety (*15*−*17*). If the incoming dNTP were replaced by an rNTP in those structures, the 2′-OH of the rNTP would clash with the side chain, or backbone, of the "steric gate" residue. This structural prediction is supported by the fact that a DNA polymerase can incorporate rNTPs into DNA as efficiently as dNTPs after the "steric gate" residue is mutated to a residue with a small side chain, e.g., Ala or Gly (*6*, *8*, *9*, *13*, *18*). Unfortunately, the E·DNA·rNTP ternary structures of any DNA polymerases and their "steric gate" mutants have not been solved yet. Thus, the structural basis for rNTP discrimination by a DNA polymerase has not been unambiguously established.

In this paper, we chose to investigate the sugar selectivity of *Sulfolobus solfataricus* P2 DNA polymerase IV (Dpo4), a model Y-family DNA polymerase. The Y-family DNA polymerases, which have been identified in all three domains of life (*19*), bypass DNA lesions in an error-prone or error-free manner, lack intrinsic proofreading exonuclease activities, and catalyze DNA synthesis with low fidelity and poor processivity (*20*−*26*). Structurally, each Y-family enzyme contains the typical finger, thumb, and palm domains found in all structurally known DNA polymerases (*17*, *27*−*32*). Interestingly, a fourth domain, designated as the "little finger" domain, is tethered to the small thumb domain via a linker and is only present in the Y-family enzymes (*16*). In Dpo4, the little finger and thumb domains bind to DNA and fit into its major and minor grooves, respectively. The palm domain contains three highly conserved carboxylate residues that bind two Mg^{2+} ions at the active site. The small finger domain contacts an

[†]This work was supported by National Science Foundation Grant MCB-0960961 (to Z.S.) and National Institutes of Health Grant ES009127 (to Z.S.). S.M.S. was supported by an American Heart Association Great River Affiliate predoctoral fellowship (Grant GRT00014861). J.D.F. was supported by a postdoctoral fellowship from Pulmonary National Institutes of Health Training Grant 5T32HL007946 (PI: Mark D. Wewers).

*To whom correspondence should be addressed. Tel: (614) 688-3706. Fax: (614) 292-6773. E-mail: suo.3@osu.edu.

[1]Abbreviations: BSA, bovine serum albumin; Dpo4, *Sulfolobus solfataricus* P2 DNA polymerase IV; dNTP, deoxyribonucleoside 5′-triphosphate; PAGE, polyacrylamide gel electrophoresis; NTP, nucleoside 5′-triphosphate; rNTP, ribonucleoside 5′-triphosphate; RT, reverse transcriptase.

Published on Web 10/25/2010

Table 1: DNA Substrates

D-1	5′-CGCAGCCGTCCAACCAACTCA-3′ 3′-GCGTCGGCAGGTTGGTTGAGTAGCAGCTA-GGTTACGGCAGG-5′
D-6	5′-CGCAGCCGTCCAACCAACTCA-3′ 3′-GCGTCGGCAGGTTGGTTGAGTGGCAGCTA-GGTTACGGCAGG-5′
D-7	5′-CGCAGCCGTCCAACCAACTCA-3′ 3′-GCGTCGGCAGGTTGGTTGAGTTGCAGCTA-GGTTACGGCAGG-5′
D-8	5′-CGCAGCCGTCCAACCAACTCA-3′ 3′-GCGTCGGCAGGTTGGTTGAGTCGCAGCTA-GGTTACGGCAGG-5′
D-1′	5′-CGCAGCCGTCCAACCAACTCA-3′ 3′-GCGTCGGCAGGTTGGTTGAGTAACAGCTA-GGTTACGGCAGG-5′
BE2	5′-TTGAGTTGCAACTCAA-3′ 3′-AACTCAACGTTGAGTT-5′

incoming dNTP but lacks the O and O_1 helices which perform fidelity checking in the high-fidelity DNA polymerases (*33*). The side chains surrounding the nascent base pair are small and hydrophobic, rather than the large and positively charged side chains present in other DNA polymerases. The active site of Dpo4 is relatively loose and solvent accessible when compared to the active sites of replicative DNA polymerases in the presence of DNA and a nucleotide (*16*). These structural features help Dpo4 to accommodate bulky DNA lesions but contribute to its low fidelity when replicating both undamaged and damaged DNA (*20*−*26*). Thus, it is possible that unfaithful Dpo4 could incorporate rNTPs efficiently. Here we utilized protein engineering and kinetic methods to investigate the sugar selectivity of Dpo4. Our results showed that Dpo4, like other Y-family members, uses a "steric gate" residue to discriminate against rNTPs.

MATERIALS AND METHODS

Materials. Reagents were purchased from the following companies: OptiKinase from USB; [γ-^{32}P]ATP from MP Biomedicals; rNTPs and dNTPs from GE Healthcare.

Protein Preparation. The mutation Y12A was introduced into the plasmid containing the full-length wild-type Dpo4 via QuikChange site-directed mutagenesis kit (Stratagene). The full-length wild-type Dpo4 and the Y12A Dpo4 mutant were expressed in *Escherichia coli* and purified as previously described (*20*).

Synthetic Oligonucleotides. The DNA substrates listed in Table 1 were purchased from Integrated DNA Technologies. All DNA substrates were purified by denaturing polyacrylamide gel electrophoresis (PAGE). The concentration of each DNA oligomer was determined by the UV absorbance at 260 nm. Each primer was 5′-^{32}P-labeled by incubating it with OptiKinase and [γ-^{32}P]ATP for 3 h at 37 °C. The 5′-^{32}P-labeled primer was annealed to an unlabeled DNA template at a molar ratio of 1.00:1.15. This mixture was first heat denatured at 95 °C for 2 min and then cooled slowly to room temperature over several hours.

Buffers. All pre-steady-state kinetic assays, if not specified, were performed in optimized reaction buffer R (50 mM HEPES, pH 7.5 at 37 °C, 5 mM $MgCl_2$, 50 mM NaCl, 0.1 mM EDTA, 5 mM DTT, 10% glycerol, and 0.1 mg/mL BSA) (*20*). All given concentrations were final after mixing all solutions.

Primer Extension Assays. The 5′-^{32}P-labeled DNA substrate D-1 (30 nM) was preincubated with either the wild-type Dpo4 or the Y12A Dpo4 mutant (120 nM) and then reacted with either all four dNTPs or rNTPs (100 μM each) or individual dNTPs or rNTPs (100 μM) at 37 °C for 2 min (or for various times during running-start experiments) in buffer R. Reactions were terminated with 0.37 M EDTA and then analyzed by denaturing PAGE (17% acrylamide, 8 M urea). The gels were visualized using a Typhoon TRIO (GE Healthcare).

Measurement of Nucleotide Incorporation Efficiency and Fidelity. Single-turnover nucleotide incorporation assays were employed to obtain the k_p and $K_{d,NTP}$ as previously described (*20*). Briefly, a preincubated solution of enzyme (120 nM) and 5′-radiolabeled DNA (30 nM) in buffer R was mixed with increasing concentrations of a single nucleotide. The reactions were terminated after various reaction times using 0.37 M EDTA. Reaction products were analyzed by denaturing PAGE (17% acrylamide, 8 M urea) and quantitated with a Typhoon TRIO (GE Healthcare). The time course of product formation at each nucleotide concentration was fit to a single-exponential equation (eq 1):

$$[\text{product}] = A[1 - \exp(-k_{obs}t)] \quad (1)$$

where k_{obs} is the observed reaction rate constant and A is the reaction amplitude. Next, the plot of the k_{obs} versus the nucleotide concentration was fit to a hyperbolic equation (eq 2):

$$k_{obs} = k_p[\text{NTP}]/\{[\text{NTP}] + K_{d,\text{NTP}}\} \quad (2)$$

where k_p is the maximum nucleotide incorporation rate constant and the $K_{d,NTP}$ is the equilibrium dissociation constant for the ternary complex (Dpo4·DNA·NTP). From these kinetic parameters, the ribonucleotide incorporation efficiency ($k_p/K_{d,NTP}$) was calculated. The ribonucleotide incorporation fidelity was also calculated using the following equation (eq 3):

$$\text{fidelity} = (k_p/K_{d,\text{NTP}})_{\text{mismatched}}/[(k_p/K_{d,\text{NTP}})_{\text{mismatched}} + (k_p/K_{d,\text{NTP}})_{\text{matched}}] \quad (3)$$

Determination of Sugar Selectivity. The sugar selectivity for a specific DNA substrate was determined for both the wild-type Dpo4 and the Y12A mutant using a nucleotide incorporation efficiency ratio (eq 4):

$$\text{sugar selectivity} = (k_p/K_d)_{\text{dNTP}}/(k_p/K_d)_{\text{rNTP}} \quad (4)$$

where $(k_p/K_d)_{dNTP}$ is the dNTP incorporation efficiency and $(k_p/K_d)_{rNTP}$ is the rNTP incorporation efficiency (*14*).

RESULTS

Reduced rNTP Discrimination by the Y12A Dpo4 Mutant. Sequence alignment of the Y-family DNA polymerases shows that Dpo4 possesses a potential "steric gate" residue Tyr12 (Supporting Information Figure 1). This putative "steric gate" residue was mutated to Ala through site-directed mutagenesis, and the single residue mutant protein was expressed and purified as described for the wild-type Dpo4 (Materials and Methods) (*20*). To test the impact of the Y12A mutation on the ability of Dpo4 to discriminate against rNTPs, running start assays using a DNA substrate D-1 (Table 1) were individually performed with the wild-type Dpo4 and its Y12A mutant at 37 °C. In the presence of four dNTPs, the wild-type Dpo4 extended primer 21-mer to the 5′-end of DNA template 41-mer before 0.6 min (Figure 1). The Y12A Dpo4 mutant also synthesized full-length products before 4 min, suggesting that the efficiency of dNTP incorporation was reduced by about 7-fold (4 min divided by 0.6 min) relative to the dNTP incorporation efficiency of the

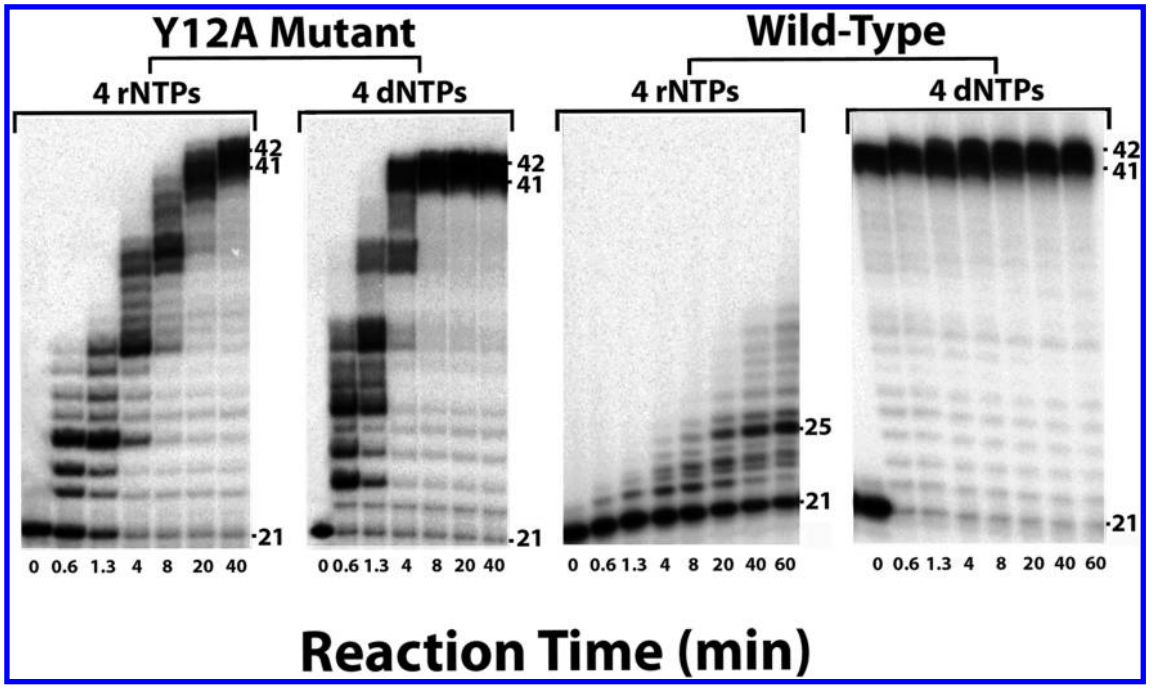

FIGURE 1: Running start assays for the wild-type Dpo4 and the Y12A Dpo4 mutant at 37 °C. A preincubated solution of enzyme (120 nM) and 5′-radiolabeled DNA substrate D-1 (30 nM) was rapidly mixed with all four rNTPs or dNTPs (100 μM each) for various reaction times before being quenched with 0.37 M EDTA. Sizes of important products are denoted on the right side of each image.

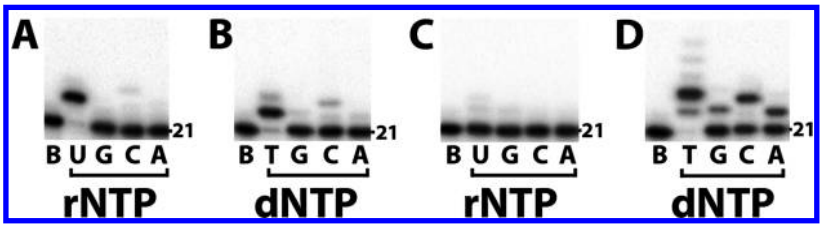

FIGURE 2: Single nucleotide incorporation assays at 37 °C. A preincubated solution of enzyme (120 nM) and 5′-radiolabeled DNA D-1 (30 nM) was rapidly reacted with the indicated nucleotide (100 μM) for 2 min before being quenched with 0.37 M EDTA. Some reactions were catalyzed by the Y12A Dpo4 mutant in the presence of an rNTP (A) or a dNTP (B) while others were catalyzed by the wild-type Dpo4 in the presence of an rNTP (C) or a dNTP (D). "'B" denotes that no enzyme was added to the reaction. The primer's size is on the right side of each image.

wild-type Dpo4 (Figure 1). In contrast to dNTP incorporation, the wild-type Dpo4 incorporated only approximately five rNTPs after 4 min with no full-length product observed within 1 h and was thus highly discriminatory against incoming rNTPs (Figure 1). Interestingly, the Y12A Dpo4 mutant was able to incorporate all four rNTPs and extended the DNA primer 21-mer to full-length products within 20 min (Figure 1). Moreover, the DNA−RNA hybrid products were reduced to the DNA primer 21-mer after alkaline degradation (Supporting Information Figure 2). Thus, the Y12A mutation caused Dpo4 to lose most of its ability to discriminate against rNTPs and synthesized 20- and 21-nucleotide RNA oligomers with a reasonable velocity. Overall, the Y12A Dpo4 mutant was approximately 5-fold (20 min divided by 4 min) less efficient when incorporating rNTPs over dNTPs to form full-length products (Figure 1). The 42-mer products in Figure 1 were likely derived from blunt-end addition (*25*). To examine if the wild-type Dpo4 and the Y12A mutant preferentially incorporated a matched or a mismatched rNTP opposite a DNA template base, single nucleotide incorporation assays were performed for 2 min at 37 °C in the presence of D-1 (Table 1). The resulting gel images are shown in Figure 2. Clearly, the Y12A Dpo4 mutant preferred to incorporate matched UTP or correct dTTP opposite the templating base dA with minimal incorporations of mismatched rNTPs or incorrect dNTPs (Figure 2). In comparison, the wild-type Dpo4 incorporated very small amounts of UTP and rGTP but incorporated all four dNTPs with a preference for correct dTTP. The latter observation is consistent with our previous kinetic results where Dpo4 displays low fidelity (10^{-3} to 10^{-4}) when incorporating dNTPs into undamaged DNA at 37 °C (*20*).

Sugar Selectivity of the Wild-Type Dpo4 and the Y12A Dpo4 Mutant. To quantitatively analyze the sugar selectivity of a DNA polymerase, the incorporation efficiencies of each dNTP and its corresponding rNTP were determined. Under single-turnover reaction conditions, we have previously determined the incorporation efficiency of each of the four correct dNTP incorporations into the corresponding D-1, D-6, D-7, or D-8 DNA substrate (Table 1) catalyzed by the wild-type Dpo4 at 37 °C (*20*). By employing the same kinetic assays, we individually determined the rNTP incorporation efficiencies with the wild-type Dpo4 as well as dNTP or rNTP incorporation efficiencies with the Y12A Dpo4 mutant. For example, a preincubated solution of the Y12A Dpo4 mutant (120 nM) and 5′-radiolabeled D-7 (Table 1) was rapidly mixed with rATP (50−1200 μM), and these reactions were quenched by 0.37 M EDTA after various reaction times. The gel image of a time course of rATP

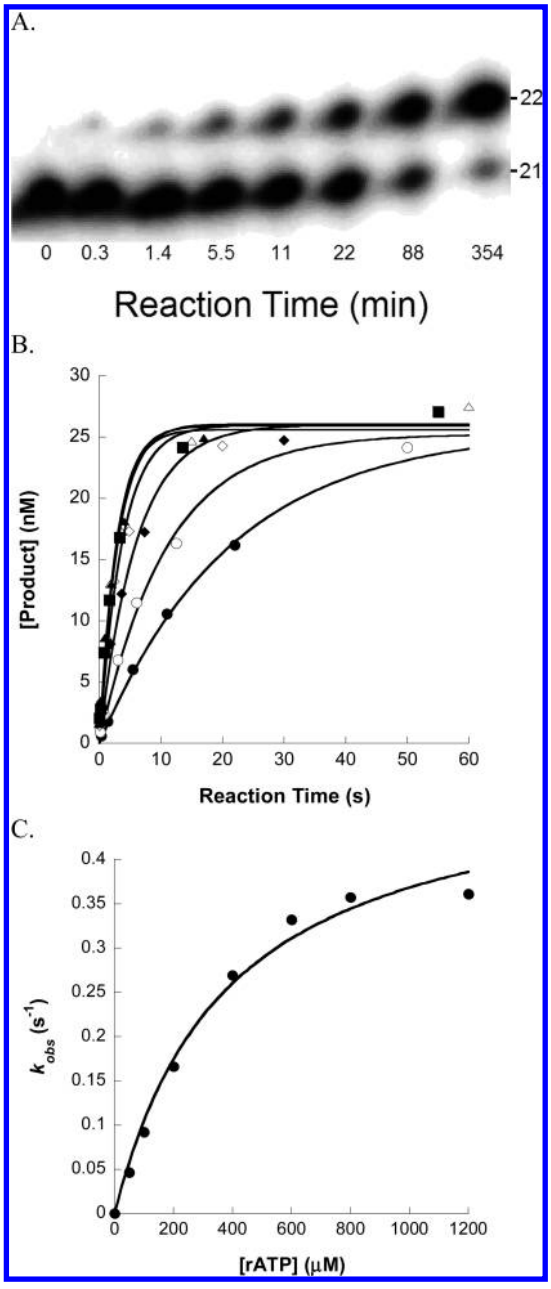

FIGURE 3: Matched rATP incorporation into DNA substrate D-7 (Table 1) catalyzed by the Y12A Dpo4 mutant at 37 °C. A preincubated solution of the Y12A Dpo4 mutant (120 nM) and 5′-radiolabeled D-7 (30 nM) was rapidly mixed with increasing concentrations of rATP before being quenched by 0.37 M EDTA at various reaction times. (A) Gel image of the time course of the incorporation of 50 μM rATP. (B) Plots of product concentration versus reaction time at specific rATP concentrations (50 μM, ●; 100 μM, ○; 200 μM, ◆; 400 μM, ◇; 600 μM, ▲; 800 μM, Δ; 1200 μM, ■). Each time course was fit to eq 1 to obtain k_{obs} (Materials and Methods). (C) Plot of k_{obs} values as a function of rATP concentrations. The data were fit to eq 2 (Materials and Methods) to obtain a k_p of 0.51 ± 0.04 s^{-1} and a $K_{d,rATP}$ of 400 ± 70 μM (Table 2).

incorporation is shown in Figure 3A. At each rATP concentration, the plot of product formation as a function of time was fit to eq 1 (Materials and Methods) to obtain the k_{obs} values (Figure 3B). Next, the k_{obs} was plotted against the corresponding rATP concentration (Figure 3C), and the plot was fit to eq 2 (Materials and Methods) to obtain the maximum nucleotide incorporation rate (k_p = 0.51 ± 0.04 s^{-1}) and the equilibrium dissociation constant ($K_{d,rATP}$ = 400 ± 70 μM) for rATP (Table 2 and Figure 3C). Recently, K. A. Johnson and co-workers have used stopped-flow and computer simulation methods to investigate dNTP incorporation catalyzed by T7 phage DNA polymerase and found that the $K_{d,dNTP}$ value obtained from single-turnover kinetic assays does not represent the true nucleotide ground state binding affinity due to protein conformational changes prior to catalysis (*34*). By monitoring real-time fluorescence resonance energy transfer signal changes, we have discovered that the four domains in Dpo4 undergo synchronized conformational changes induced by correct dNTP binding (*35*). If rNTP binding induces similar protein conformational changes in Dpo4 as dNTP (*35*), the above measured $K_{d,ATP}$ will be considered an apparent $K_{d,ATP}$.

Using the measured k_p and $K_{d,rATP}$ values, we then calculated rATP incorporation efficiency ($k_p/K_{d,rATP}$ = 1.3 × 10^{-3} μM^{-1} s^{-1}) and sugar selectivity ($(k_p/K_d)_{dATP}/(k_p/K_d)_{rATP}$ = 3) for the Y12A Dpo4 mutant (Table 2). Opposite template bases dA, dG, and dC, the sugar selectivity values were measured under the same single-turnover reaction conditions and were determined to be 30, 12, and 4, respectively. In comparison, the sugar selectivity values for the wild-type Dpo4 were also determined, and they are 20500, 18333, 13448, and 5500 (Table 2) for dTTP/UTP, dGTP/rGTP, dATP/rATP, and dCTP/rCTP, respectively. Comparing these sugar selectivity values in Table 2, the Y12A mutation significantly decreased the sugar selectivity of Dpo4 (Figure 4). The extremely low rNTP incorporation efficiencies relative to those of correct dNTPs with the wild-type Dpo4 (Table 2) are consistent with the product formation patterns observed in Figure 1: incorporation of rNTPs catalyzed by the wild-type Dpo4 was extremely inefficient while dNTPs were rapidly incorporated. When comparing the kinetic parameters (Table 2) of the wild-type Dpo4 and its Y12A mutant, the mutation caused moderate to significant changes in both k_p and $K_{d,dNTP}$ values for dNTP incorporation, which led to 3-, 32-, 10-, and 19-fold decreases in dTTP, dGTP, dCTP, and dATP incorporation efficiencies, respectively. The difference in dNTP incorporation efficiencies correlated well to the slower formation of the full-length DNA products synthesized by the Y12A mutant than by the wild-type Dpo4 (Figure 1). In addition, the Y12A Dpo4 mutant incorporated rNTPs and dNTPs with very different kinetic parameters. Relative to dNTP incorporation, the k_p values decreased by ~9-fold for all matched rNTP incorporations, the $K_{d,rNTP}$ values increased by ~2-fold for pyrimidine nucleotides (i.e., UTP/dTTP, rCTP/dCTP), and the $K_{d,rNTP}$ values decreased by about 2-fold for purine nucleotides (i.e., rGTP/dGTP, rATP/dATP). These changes in the kinetic parameters led to rNTP incorporation with 3−30-fold lower efficiencies than the corresponding dNTP incorporation (Table 2), resulting in the slower DNA primer extension in the presence of rNTPs relative to dNTPs (Figure 1).

Fidelity of DNA-Dependent RNA Polymerase Activity of the Y12A Dpo4 Mutant. Figure 1 shows that the Y12A Dpo4 mutant possesses a DNA-dependent RNA polymerase activity in addition to the DNA-dependent DNA polymerase activity. To determine the fidelity of this DNA-dependent RNA polymerase activity, the kinetic parameters (Table 3) of mismatched rNTP incorporations into DNA substrate D-1, e.g., rATP incorporation (Supporting Information Figure 3), were determined under single-turnover reaction conditions. Opposite templating base dA, both k_p and $k_p/K_{d,rNTP}$ values of mismatched rNTPs are 2−3 orders of magnitude lower than those of matched UTP while the difference in $K_{d,rNTP}$ values is within 2-fold (Table 3). The calculated fidelity for the DNA-dependent RNA

Table 2: Kinetic Parameters of Matched rNTP or dNTP Incorporation into DNA Catalyzed by the Wild-Type Dpo4 or Its Y12A Mutant at 37 °C

Dpo4	DNA substrate	nucleotide	k_p (s^{-1})	K_d (μM)	k_p/K_d (μM^{-1} s^{-1})	sugar selectivity[a]
wild type	D-1	dTTP[b]	9.4 ± 0.3	230 ± 17	4.1×10^{-2}	
	D-1	UTP	$(4.0 \pm 1.0) \times 10^{-3}$	2158 ± 779	2.0×10^{-6}	20500
	D-8	dGTP[b]	9.4 ± 0.2	171 ± 15	5.5×10^{-2}	
	D-8	rGTP	$(2.9 \pm 0.2) \times 10^{-3}$	980 ± 166	3.0×10^{-6}	18333
	D-6	dCTP[b]	7.6 ± 0.2	70 ± 8	1.1×10^{-1}	
	D-6	rCTP	$(6.4 \pm 0.6) \times 10^{-2}$	3111 ± 419	2.0×10^{-5}	5500
	D-7	dATP[b]	16 ± 0.9	206 ± 46	7.8×10^{-2}	
	D-7	rATP	$(8.1 \pm 0.6) \times 10^{-3}$	1405 ± 172	5.8×10^{-6}	13448
Y12A	D-1	dTTP	4.5 ± 0.5	300 ± 90	1.5×10^{-2}	
	D-1	UTP	$(3.3 \pm 0.4) \times 10^{-1}$	600 ± 200	5.5×10^{-4}	30
	D-8	dGTP	$(9.4 \pm 0.9) \times 10^{-1}$	540 ± 100	1.7×10^{-3}	
	D-8	rGTP	$(1.1 \pm 0.1) \times 10^{-1}$	270 ± 40	4.1×10^{-3}	4
	D-6	dCTP	4.9 ± 0.2	460 ± 45	1.1×10^{-2}	
	D-6	rCTP	0.7 ± 0.1	800 ± 300	8.8×10^{-4}	12
	D-7	dATP	3.7 ± 0.5	900 ± 200	4.1×10^{-3}	
	D-7	rATP	$(5.1 \pm 0.4) \times 10^{-1}$	400 ± 70	1.3×10^{-3}	3

[a]Calculated as $(k_p/K_d)_{dNTP}/(k_p/K_d)_{rNTP}$. [b]Kinetic parameters are from ref 20.

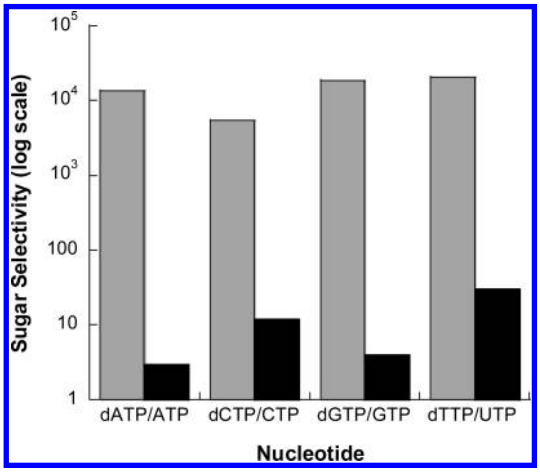

FIGURE 4: Comparison of sugar selectivity values (Table 2) between the wild-type Dpo4 (gray bar) and the Y12A Dpo4 mutant (black bar).

polymerase activity of the Y12A Dpo4 mutant is in the range of 10^{-3} to 10^{-4} (Table 3). Notably, the Y12A Dpo4 mutant misincorporated rCTP 14- and 3-fold more efficiently than rATP and rGTP, respectively (Table 3). Since the 5′-base from the templating base dA in D-1 is dG (Table 1), the enhanced misincorporation of rCTP was probably due to rNTP-stabilized misalignment as observed with dNTP misincorporation catalyzed by the wild-type Dpo4 (*20*). This hypothesis was proven to be correct based on the fact that rCTP misincorporation efficiency (1.1×10^{-7} μM^{-1} s^{-1}) is 21-fold lower when the 5′-base dG (D-1) from the templating base dA was changed to dA (D-1′) (Table 3).

Blunt-End rNTP Addition Catalyzed by the Y12A Dpo4 Mutant. The 42-mer products in Figure 1 indicate that the Y12A Dpo4 mutant was able to catalyze a blunt-end rNTP addition onto an RNA/DNA duplex 41/41-mer as it incorporated a dNTP onto the blunt-end DNA/DNA duplex 41/41-mer. To examine how slow the blunt-end addition activity is, we measured the rate constant for rNTP incorporation onto BE2 (Table 1) catalyzed by the Y12A Dpo4 mutant. This mutant was able to incorporate a small amount of rATP (~2 nM) after 2 h (Figure 5A). The k_{obs} was determined to be $(2.9 \pm 0.4) \times 10^{-5}$ s^{-1} when the rATP concentration was 600 μM (Figure 5B). This value is 120−207-fold lower than the k_p values ($3.5-6 \times 10^{-3}$ s^{-1}) for the blunt-end dATP addition catalyzed by the wild-type Dpo4 (*25*). Under the same reaction conditions as in Figure 5A, there were no detectable blunt-end additions of either rCTP, rGTP, or UTP (data not shown). Thus, blunt-end rNTP additions onto a DNA/DNA duplex are much less efficient than the corresponding blunt-end dNTP additions, and rATP, like dATP, was the preferred nucleotide for this activity due to strong intrahelical base stacking interactions between nucleobase adenine and blunt-end DNA (*25*).

DISCUSSION

Kinetic Basis for Sugar Selectivity of Dpo4. Sequence alignment of the Y-family DNA polymerases (Supporting Information Figure 1) indicates a conserved Tyr or Phe residue which likely serves as the "steric gate" in the discrimination against rNTPs. Mutation of Phe12 of *Sulfolobus acidocaldarius* Dbh to Ala, which possesses a much smaller side chain than Phe, decreases the sugar selectivity ($(k_p/K_d)_{dGTP}/(k_p/K_d)_{rGTP}$) of this Y-family member from 3400 to 4 for rGTP/dGTP (*9*). Similarly, the mutation of Phe13 of *E. coli* DinB to slightly less bulky Val has a modest effect on its sugar selectivity which drops from 10^5 to 10^3 (*36*). Since Dpo4 belongs to the same DinB subfamily, one can predict that the Y12A mutation will likely relax Dpo4's discrimination against rNTPs. This prediction was confirmed by the product formation patterns in Figure 2 which directly demonstrate when opposite the templating base dA, UTP was as good a nucleotide substrate as dTTP to the Y12A Dpo4 mutant and a much better substrate to the Y12A mutant than to the wild-type Dpo4. This prediction was also confirmed by our kinetically determined sugar selectivity values which show that the sugar selectivity decreased from the range of 5500−20500 for the wild-type Dpo4 to 3−30 for the Y12A Dpo4 mutant, depending on the identity of a nascent base pair (Table 2 and Figure 4). The kinetic basis for the significant decrease in sugar selectivity is that the Y12A mutation dramatically enhanced rNTP incorporation efficiency ($(k_p/K_d)_{rNTP}$) by an average of 221-fold while decreasing correct dNTP incorporation efficiency ($(k_p/K_d)_{dNTP}$) by an average of 9-fold, leading to a calculated reduction of sugar selectivity by 1989-fold. Moreover, the difference between the average efficiency for dNTP (8.0×10^{-3} μM^{-1} s^{-1}) and rNTP incorporation (1.7×10^{-3} μM^{-1} s^{-1}) for the Y12A Dpo4 mutant is only 5-fold while it is 9200-fold for the

Table 3: Kinetic Parameters of Mismatched rNTP Incorporation into a DNA Substrate with 5′-dG (D-1) or 5′-dA (D-1′) from the Templating Base dA (Table 1) Catalyzed by the Y12A Dpo4 Mutant at 37 °C

rNTP	k_p (s^{-1})	$K_{d,rNTP}$ (μM)	$k_p/K_{d,rNTP}$ (μM^{-1} s^{-1})	rNTP incorporation fidelity[b]
DNA substrate D-1				
UTP[a]	$(3.3 \pm 0.4) \times 10^{-1}$	600 ± 200	5.5×10^{-4}	
rATP	$(2.2 \pm 0.1) \times 10^{-4}$	1292 ± 154	1.7×10^{-7}	3.1×10^{-4}
rCTP	$(11.0 \pm 0.4) \times 10^{-4}$	489 ± 33	2.3×10^{-6}	4.2×10^{-3}
rGTP	$(5.3 \pm 0.5) \times 10^{-4}$	793 ± 152	6.7×10^{-7}	1.2×10^{-3}
DNA substrate D-1′				
rCTP	$(9.8 \pm 1.9) \times 10^{-5}$	903 ± 344	1.1×10^{-7}	undetermined

[a]Kinetic parameters for matched UTP are from Table 2. [b]Calculated as $(k_p/K_d)_{mismatched\ rNTP}/[(k_p/K_d)_{matched\ rNTP} + (k_p/K_d)_{mismatched\ rNTP}]$.

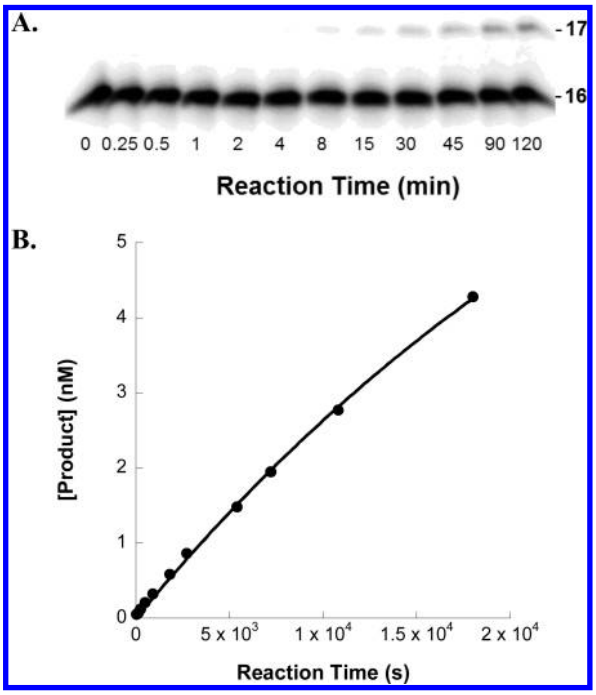

FIGURE 5: Blunt-end rATP additions onto DNA substrate BE2 (Table 1) catalyzed by the Y12A Dpo4 mutant at 37 °C. (A) Gel image of the time course of rATP (600 μM) incorporation. (B) Plot of product concentrations in (A) as a function of reaction times. The time course was fit to eq 1 (Materials and Methods) to yield a k_{obs} of $(2.9 \pm 0.4) \times 10^{-5}$ s^{-1}.

wild-type Dpo4. Thus, the small side chain of Ala12 allowed Dpo4 to incorporate rNTPs almost as efficiently as dNTPs. The 5-fold difference between dNTP and rNTP incorporation efficiency for the Y12A Dpo4 mutant was mainly contributed by the difference in k_p values (9-fold) (Table 2). In contrast, the average k_p value difference between dNTP and rNTP incorporations catalyzed by the wild-type Dpo4 was 1925-fold while the average K_d difference is only 17-fold (Table 2). These kinetic data suggested that the Y12A mutation of Dpo4 mainly affected catalysis (k_p), rather than the nucleotide binding step (K_d). The kinetic insights into the sugar selectivity of Dpo4 may shed light on how human Y-family DNA polymerases discriminate against ribonucleotides *in vivo*, especially when dNTP pools are low and rNTP pools are high (*14*), as their proposed "steric gate" residues are either Phe or Tyr (Supporting Information Figure 1).

To obtain a structural sense on how Dpo4 discriminates against an incoming rNTP, we modeled rATP into the binding site of dATP by swapping the ribose rings between Dpo4-bound dATP (PDB 2AGQ) and an N^5-CAIR synthetase-bound rATP (PDB 3ETH) (Supporting Information Figure 4) (*37*, *38*). The adenine base and the triphosphate were not modified. The C1′, C4′, and C3′ atoms of the rATP (PDB 3ETH) occupied the same positions as those corresponding atoms in the Dpo4-bound dATP (PDB 2AGQ). Unfortunately, the O2′ of the incoming rATP and the side chain of Tyr12 are at least 0.7 Å too close to avoid a steric clash based on van der Waals atomic radii (Supporting Information Figure 4B). In solution, the side chain of Tyr12 must move away from an incoming rATP in order for Dpo4 to bind and incorporate this rATP. This movement will require more energy and may explain why the matched rNTP incorporation efficiencies with the wild-type Dpo4 were significantly lower than the matched rNTP incorporation efficiencies with the Y12A Dpo4 mutant (Table 2).

DNA-Dependent RNA Polymerase Activity of the Y12A Dpo4 Mutant. In addition to an intrinsic DNA-dependent DNA polymerase activity, the Y12A Dpo4 mutant was able to incorporate at least 20 consecutive rNTPs into the DNA substrate D-1 21/41-mer (Figure 1) and displayed a DNA-dependent RNA polymerase activity. Interestingly, this activity did not reach its upper limit since longer RNA polymers were synthesized by the Y12A Dpo4 mutant with shorter DNA primers (data not shown). In comparison, the binary and ternary crystal structures of Dpo4 have shown that the DNA binding cleft of Dpo4 is about eight base pairs in length, and the bound DNA/DNA duplex is completely in the B-type conformation (*16*, *31*). Thus, the DNA binding cleft of the Y12A Dpo4 mutant can accommodate both DNA/DNA (B-type) and RNA/DNA (A-type) helices during polymerization. Similarly, the F12A Dbh mutant has been found to be capable of performing at least 10 successive rNTP insertions into a DNA/DNA duplex 13/23-mer (*9*), suggesting that Dbh, like its Y-family homologue Dpo4, can readily bind both A- and B-type helices at its flexible DNA binding cleft. This is not surprising considering that the Y-family DNA polymerases are known to accommodate DNA containing bulky and helix-distorting lesions during translesion DNA synthesis. The ternary crystal structures of both Dpo4 (*16*, *31*) and Dbh (*30*) demonstrate that the DNA binding cleft of either Y-family enzyme is formed by a polymerase core (palm, thumb, and finger domains) and a little finger domain; their physical connection is through a 14 amino acid residue linker. This linker likely increases the flexibility of the DNA binding cleft by facilitating the repositioning of the little finger domain relative to the polymerase core, depending on the conformation of bound DNA helix (A- or B-type). This hypothesis is supported by the modeling result revealed in Supporting Information Figure 5: only a portion (five base pairs) of the B-type DNA/DNA duplex (eight base pairs) in the ternary structure of Dpo4 can be replaced by the same sized A-type

RNA/DNA duplex without steric hindrance of the little finger domain. Interestingly, unlike the Y-family enzymes Dpo4 and Dbh, DNA polymerases from other families do not possess the little finger domain and the linker; therefore, their DNA binding clefts are predicted to be relatively stringent. A stringent DNA cleft may not tolerate pure A-type helices and may limit the polymerase to synthesize a long RNA polymer opposite a DNA template. Consistently, the "steric gate" mutants of those non-Y-family DNA polymerases have been found to only add approximately four to six rNTPs to a DNA/DNA duplex (*6*, *8*, *39*−*42*). In addition, these studies also indicate that the DNA binding clefts of those non-Y-family DNA polymerase mutants can simultaneously tolerate a stretch (four to six base pairs) of RNA/DNA helix from the primer 3′-terminus and a stretch of DNA/DNA helix near the primer 5′-terminus. Interestingly, this covalently linked A-type and B-type duplex conformation has been observed in the ternary crystal structures of those non-Y-family DNA polymerases in complex with DNA and dNTP which show that a portion (about four base pairs) of the double-stranded DNA duplex next to the primer 3′-terminus is in an A-like conformation while the rest of the DNA duplex is in the B-type conformation (*33*, *43*−*45*).

Interestingly, the fidelity of rNTP incorporation into D-1 (Table 1) catalyzed by the Y12A Dpo4 mutant was measured to be in the range of 10^{-3} to 10^{-4} (Table 3), which is identical to the fidelity range for the DNA-dependent DNA polymerase activity of the wild-type Dpo4 (*20*). This suggests that the DNA-dependent RNA polymerase activity of the Y12A Dpo4 mutant is as error prone as its intrinsic DNA-dependent DNA polymerase activity. Although slow, the DNA-dependent RNA polymerase activity of the Y12A Dpo4 mutant catalyzed blunt-end rNTP and dNTP additions (Figure 1), and the predominant blunt-end rNTP addition event is single rATP incorporation (Figure 5). These observations mirror what we have observed with the blunt-end dNTP additions catalyzed by the wild-type Dpo4 (*25*). Taken together, we conclude that the DNA-dependent RNA polymerase activity and DNA-dependent DNA polymerase activity of the Y12A Dpo4 mutant are mechanistically similar.

SUPPORTING INFORMATION AVAILABLE

Amino acid sequence alignment (Figure 1), alkaline degradation of full-length RNA extension product catalyzed by the Y12A Dpo4 mutant (Figure 2), kinetic plots of the mismatched rATP incorporation at 37 °C catalyzed by the Y12A Dpo4 mutant (Figure 3), active site model comparison of the wild-type Dpo4 with dATP or rATP (Figure 4), and model of the Y12A Dpo4 mutant in complex with RNA primer/DNA template hybrid and rATP (Figure 5). This material is available free of charge via the Internet at http://pubs.acs.org.

REFERENCES

1. Traut, T. W. (1994) Physiological concentrations of purines and pyrimidines. *Mol. Cell. Biochem. 140*, 1–22.
2. Ferraro, P., Franzolin, E., Pontarin, G., Reichard, P., and Bianchi, V. (2010) Quantitation of cellular deoxynucleoside triphosphates. *Nucleic Acids Res. 38*, e85.
3. Nick McElhinny, S. A., Watts, B. E., Kumar, D., Watt, D. L., Lundstrom, E. B., Burgers, P. M., Johansson, E., Chabes, A., and Kunkel, T. A. (2010) Abundant ribonucleotide incorporation into DNA by yeast replicative polymerases. *Proc. Natl. Acad. Sci. U.S.A. 107*, 4949–4954.
4. Fowler, J. D., and Suo, Z. (2006) Biochemical, structural, and physiological characterization of terminal deoxynucleotidyl transferase. *Chem. Rev. 106*, 2092–2110.
5. Joyce, C. M. (1997) Choosing the right sugar: how polymerases select a nucleotide substrate. *Proc. Natl. Acad. Sci. U.S.A. 94*, 1619–1622.
6. Astatke, M., Ng, K., Grindley, N. D., and Joyce, C. M. (1998) A single side chain prevents *Escherichia coli* DNA polymerase I (Klenow fragment) from incorporating ribonucleotides. *Proc. Natl. Acad. Sci. U.S.A. 95*, 3402–3407.
7. Patel, P. H., and Loeb, L. A. (2000) Multiple amino acid substitutions allow DNA polymerases to synthesize RNA. *J. Biol. Chem. 275*, 40266–40272.
8. Bonnin, A., Lazaro, J. M., Blanco, L., and Salas, M. (1999) A single tyrosine prevents insertion of ribonucleotides in the eukaryotic-type phi29 DNA polymerase. *J. Mol. Biol. 290*, 241–251.
9. DeLucia, A. M., Grindley, N. D., and Joyce, C. M. (2003) An error-prone family Y DNA polymerase (DinB homolog from *Sulfolobus solfataricus*) uses a "steric gate" residue for discrimination against ribonucleotides. *Nucleic Acids Res. 31*, 4129–4137.
10. Gao, G., Orlova, M., Georgiadis, M. M., Hendrickson, W. A., and Goff, S. P. (1997) Conferring RNA polymerase activity to a DNA polymerase: a single residue in reverse transcriptase controls substrate selection. *Proc. Natl. Acad. Sci. U.S.A. 94*, 407–411.
11. Gardner, A. F., Joyce, C. M., and Jack, W. E. (2004) Comparative kinetics of nucleotide analog incorporation by vent DNA polymerase. *J. Biol. Chem. 279*, 11834–11842.
12. Niimi, N., Sassa, A., Katafuchi, A., Gruz, P., Fujimoto, H., Bonala, R. R., Johnson, F., Ohta, T., and Nohmi, T. (2009) The steric gate amino acid tyrosine 112 is required for efficient mismatched-primer extension by human DNA polymerase kappa. *Biochemistry 48*, 4239–4246.
13. Yang, G., Franklin, M., Li, J., Lin, T. C., and Konigsberg, W. (2002) A conserved Tyr residue is required for sugar selectivity in a Pol alpha DNA polymerase. *Biochemistry 41*, 10256–10261.
14. Brown, J. A., Fiala, K. A., Fowler, J. D., Sherrer, S. M., Newmister, S. A., Duym, W. W., and Suo, Z. (2010) A novel mechanism of sugar selection utilized by a human X-family DNA polymerase. *J. Mol. Biol. 395*, 282–290.
15. Biertumpfel, C., Zhao, Y., Kondo, Y., Ramon-Maiques, S., Gregory, M., Lee, J. Y., Masutani, C., Lehmann, A. R., Hanaoka, F., and Yang, W. (2010) Structure and mechanism of human DNA polymerase eta. *Nature 465*, 1044–1048.
16. Ling, H., Boudsocq, F., Woodgate, R., and Yang, W. (2001) Crystal structure of a Y-family DNA polymerase in action: a mechanism for error-prone and lesion-bypass replication. *Cell 107*, 91–102.
17. Lone, S., Townson, S. A., Uljon, S. N., Johnson, R. E., Brahma, A., Nair, D. T., Prakash, S., Prakash, L., and Aggarwal, A. K. (2007) Human DNA polymerase kappa encircles DNA: implications for mismatch extension and lesion bypass. *Mol. Cell 25*, 601–614.
18. Cases-Gonzalez, C. E., Gutierrez-Rivas, M., and Menendez-Arias, L. (2000) Coupling ribose selection to fidelity of DNA synthesis. The role of Tyr-115 of human immunodeficiency virus type 1 reverse transcriptase. *J. Biol. Chem. 275*, 19759–19767.
19. Ohmori, H., Friedberg, E. C., Fuchs, R. P., Goodman, M. F., Hanaoka, F., Hinkle, D., Kunkel, T. A., Lawrence, C. W., Livneh, Z., Nohmi, T., Prakash, L., Prakash, S., Todo, T., Walker, G. C., Wang, Z., and Woodgate, R. (2001) The Y-family of DNA polymerases. *Mol. Cell 8*, 7–8.
20. Fiala, K. A., and Suo, Z. (2004) Pre-steady-state kinetic studies of the fidelity of *Sulfolobus solfataricus* P2 DNA polymerase IV. *Biochemistry 43*, 2106–2115.
21. Fiala, K. A., and Suo, Z. (2004) Mechanism of DNA polymerization catalyzed by *Sulfolobus solfataricus* P2 DNA polymerase IV. *Biochemistry 43*, 2116–2125.
22. Fiala, K. A., Hypes, C. D., and Suo, Z. (2007) Mechanism of abasic lesion bypass catalyzed by a Y-family DNA polymerase. *J. Biol. Chem. 282*, 8188–8198.
23. Brown, J. A., Newmister, S. A., Fiala, K. A., and Suo, Z. (2008) Mechanism of double-base lesion bypass catalyzed by a Y-family DNA polymerase. *Nucleic Acids Res. 36*, 3867–3878.
24. Sherrer, S. M., Brown, J. A., Pack, L. R., Jasti, V. P., Fowler, J. D., Basu, A. K., and Suo, Z. (2009) Mechanistic studies of the bypass of a bulky single-base lesion catalyzed by a Y-family DNA polymerase. *J. Biol. Chem. 284*, 6379–6388.
25. Fiala, K. A., Brown, J. A., Ling, H., Kshetry, A. K., Zhang, J., Taylor, J. S., Yang, W., and Suo, Z. (2007) Mechanism of template-independent nucleotide incorporation catalyzed by a template-dependent DNA polymerase. *J. Mol. Biol. 365*, 590–602.
26. Kunkel, T. A. (2004) DNA replication fidelity. *J. Biol. Chem. 279*, 16895–16898.
27. Nair, D. T., Johnson, R. E., Prakash, L., Prakash, S., and Aggarwal, A. K. (2005) Rev1 employs a novel mechanism of DNA synthesis using a protein template. *Science 309*, 2219–2222.

28. Nair, D. T., Johnson, R. E., Prakash, S., Prakash, L., and Aggarwal, A. K. (2004) Replication by human DNA polymerase-iota occurs by Hoogsteen base-pairing. *Nature 430*, 377–380.
29. Trincao, J., Johnson, R. E., Escalante, C. R., Prakash, S., Prakash, L., and Aggarwal, A. K. (2001) Structure of the catalytic core of *S. cerevisiae* DNA polymerase eta: implications for translesion DNA synthesis. *Mol. Cell 8*, 417–426.
30. Wilson, R. C., and Pata, J. D. (2008) Structural insights into the generation of single-base deletions by the Y family DNA polymerase dbh. *Mol. Cell 29*, 767–779.
31. Wong, J. H., Fiala, K. A., Suo, Z., and Ling, H. (2008) Snapshots of a Y-family DNA polymerase in replication: substrate-induced conformational transitions and implications for fidelity of Dpo4. *J. Mol. Biol. 379*, 317–330.
32. Zhou, B. L., Pata, J. D., and Steitz, T. A. (2001) Crystal structure of a DinB lesion bypass DNA polymerase catalytic fragment reveals a classic polymerase catalytic domain. *Mol. Cell 8*, 427–437.
33. Doublie, S., Tabor, S., Long, A. M., Richardson, C. C., and Ellenberger, T. (1998) Crystal structure of a bacteriophage T7 DNA replication complex at 2.2 A resolution. *Nature 391*, 251–258.
34. Tsai, Y. C., and Johnson, K. A. (2006) A new paradigm for DNA polymerase specificity. *Biochemistry 45*, 9675–9687.
35. Xu, C., Maxwell, B. A., Brown, J. A., Zhang, L., and Suo, Z. (2009) Global conformational dynamics of a Y-family DNA polymerase during catalysis. *PLoS Biol. 7*, e1000225.
36. Jarosz, D. F., Godoy, V. G., Delaney, J. C., Essigmann, J. M., and Walker, G. C. (2006) A single amino acid governs enhanced activity of DinB DNA polymerases on damaged templates. *Nature 439*, 225–228.
37. Vaisman, A., Ling, H., Woodgate, R., and Yang, W. (2005) Fidelity of Dpo4: effect of metal ions, nucleotide selection and pyrophosphorolysis. *EMBO J. 24*, 2957–2967.
38. Thoden, J. B., Holden, H. M., and Firestine, S. M. (2008) Structural analysis of the active site geometry of N5-carboxyaminoimidazole ribonucleotide synthetase from *Escherichia coli*. *Biochemistry 47*, 13346–13353.
39. Boule, J. B., Rougeon, F., and Papanicolaou, C. (2001) Terminal deoxynucleotidyl transferase indiscriminately incorporates ribonucleotides and deoxyribonucleotides. *J. Biol. Chem. 276*, 31388–31393.
40. Gardner, A. F., and Jack, W. E. (1999) Determinants of nucleotide sugar recognition in an archaeon DNA polymerase. *Nucleic Acids Res. 27*, 2545–2553.
41. Liu, S., Goff, S. P., and Gao, G. (2006) Gln(84) of moloney murine leukemia virus reverse transcriptase regulates the incorporation rates of ribonucleotides and deoxyribonucleotides. *FEBS Lett. 580*, 1497–1501.
42. Ruiz, J. F., Juarez, R., Garcia-Diaz, M., Terrados, G., Picher, A. J., Gonzalez-Barrera, S., Fernandez de Henestrosa, A. R., and Blanco, L. (2003) Lack of sugar discrimination by human Pol mu requires a single glycine residue. *Nucleic Acids Res. 31*, 4441–4449.
43. Huang, H., Chopra, R., Verdine, G. L., and Harrison, S. C. (1998) Structure of a covalently trapped catalytic complex of HIV-1 reverse transcriptase: implications for drug resistance. *Science 282*, 1669–1675.
44. Johnson, S. J., Taylor, J. S., and Beese, L. S. (2003) Processive DNA synthesis observed in a polymerase crystal suggests a mechanism for the prevention of frameshift mutations. *Proc. Natl. Acad. Sci. U.S.A. 100*, 3895–3900.
45. Li, Y., Korolev, S., and Waksman, G. (1998) Crystal structures of open and closed forms of binary and ternary complexes of the large fragment of *Thermus aquaticus* DNA polymerase I: structural basis for nucleotide incorporation. *EMBO J. 17*, 7514–7525.